NIH Public Access
Author Manuscript
Ann Neurol. Author manuscript; available in PMC 2013 October 01.

Published in final edited form as:
Ann Neurol. 2012 October ; 72(4): 517–524. doi:10.1002/ana.23747.

Neuron-to-neuron transmission of α-synuclein fibrils through axonal transport

Eric C. Freundt, PhD[1,4], **Nate Maynard, PhD**[3], **Eileen K. Clancy, PhD**[1], **Shyamali Roy, PhD**[1], **Luc Bousset, PhD**[2], **Yannick Sourigues**[2], **Markus Covert, PhD**[3], **Ronald Melki, PhD**[2], **Karla Kirkegaard, PhD**[1], and **Michel Brahic, MD, PhD**[1]

[1]Department of Microbiology and Immunology, Stanford University School of Medicine, Stanford, CA 94305-5402, USA

[2]Laboratoire d'Enzymologie et Biochimie Structurales, Centre National de la Recherche Scientifique, 91198 Gif–sur–Yvette, France

[3]Department of Bioengineering, Stanford University School of Medicine, Stanford, CA 94305-5402, USA

Abstract

Objective—The lesions of Parkinson's disease spread through the brain in a characteristic pattern that corresponds to axonal projections. Previous observations suggest that misfolded α-synuclein could behave as a prion, moving from neuron to neuron and causing endogenous α-synuclein to misfold. Here, we characterized and quantified the axonal transport of α-synuclein fibrils and showed that fibrils could be transferred from axons to second-order neurons following anterograde transport.

Methods—We grew primary cortical mouse neurons in microfluidic devices to separate soma from axonal projections in fluidically isolated microenvironments. We used live-cell imaging and immunofluorescence to characterize the transport of fluorescent α-synuclein fibrils and their transfer to second-order neurons.

Results—Fibrillar α-synuclein was internalized by primary neurons and transported in axons with kinetics consistent with slow component-b of axonal transport (fast axonal transport with saltatory movement). Fibrillar α-synuclein was readily observed in the cell bodies of second-order neurons following anterograde axonal transport. Axon-to-soma transfer appeared not to require synaptic contacts.

Interpretation—These results support the hypothesis that the progression of Parkinson's disease can be caused by neuron-to-neuron spread of α-synuclein aggregates and that the anatomical pattern of progression of lesions between axonally connected areas results from the axonal transport of such aggregates. That the transfer did not appear to be transsynaptic gives hope that α-synuclein fibrils could be intercepted by drugs during the extra-cellular phase of their journey.

Address correspondence to Michel Brahic, Department of Microbiology Immunology, Stanford University School of Medicine, Fairchild Building, 299 Campus Drive, Stanford CA 94305-5402 Ph: 650 498 7085, mbrahic@stanford.edu,.
[4]Present address: Department of Biology, The University of Tampa, Tampa, FL 33606, USA

Potential conflict of interest
Nothing to report

$watermark-text
$watermark-text
$watermark-text

$watermark-text

$watermark-text

$watermark-text

Introduction

Parkinson's disease (PD) is a common neurodegenerative disorder, second in frequency only to Alzheimer's disease. PD can cause cognitive impairment as well as movement disorders[1]. α-Synuclein is the major component of Lewy bodies and Lewy neurites, the filamentous inclusions characteristic of PD and other “synucleinopathies” such as dementia with Lewy bodies and multiple system atrophy. Besides being diagnostic of this group of diseases, the accumulation of aggregated proteins including α-synuclein is thought to play a role in neurodegeneration. α-Synuclein is a 140-amino acid protein that adopts an α-helical structure when bound to membranes but can also fold into a β-sheet-rich structure that polymerizes into fibrils and protein aggregates[2]. It has been hypothesized that aggregated α-synuclein might behave like a prion, capable of initiating misfolding and aggregation of nascent or even properly folded α-synuclein[3,4,5,6]. The prion hypothesis is supported by the observation that young mice of the M83 line, a transgenic line which overexpress the A53T mutant human α-synuclein, develop a motor disease with insoluble α-synuclein deposits in the CNS following intracerebral inoculation with brain homogenates from old M83 mice[7,8].

The lesions of PD progress along an ascending pattern that corresponds to anatomical connections between brain structures. For example, early lesions predominate in olfactory bulbs and appear to spread in an anterograde direction from there to the limbic system and the neocortex[9]. Similarly, the lesions of the substantia nigra appear to spread to the striatum, and those of the ventral tegmental area to the cortex, in both cases following anterograde axonal pathways[9]. These patterns may be interpreted as resulting from axonal transport of an “infectious”, or at least self-propagating, form of α-synuclein followed by spread to a higher order neuron. This spread could involve either lysis of the first neuron or a non-lytic unconventional secretion pathway.

Host-to-graft propagation of Lewy bodies was recently demonstrated at autopsy in PD patients who had received neuronal grafts decades earlier[10,11], an observation that has been reproduced in a mouse model[12]. However, it is not yet known whether the aggregation of α-synuclein in the grafts is due to the spread of the misfolded α-synuclein or to the spread of conditions conducive to α-synuclein aggregation. Consistent with the first scenario, the release of misfolded α-synuclein by cultured cells, including neurons, has been documented, as has the ability of cultured cell lines, including those of neural origin, to take up aggregated α-synuclein from culture medium[12-14]. Findings consistent with transmission of α-synuclein between co-cultured neurons have been reported previously, although the role of axonal transport in this transmission was not addressed[15]. In the present paper, we used microfluidic chambers to characterize the axonal transport of α-synuclein fibrils. We show that this transport proceeds with velocities characteristic of fast axonal transport with “stop and go” phases, a type of transport referred to as slow component-b of axonal transport[16,17]. Importantly, we have demonstrated the transfer of axonally transported fibrillar α-synuclein to the soma of second order neurons.

Materials and methods

Cells

The cortices of E17 mouse embryos were incubated in 0.125% trypsin in Earle's balanced salt solution for eight minutes at 37°C and re-suspended in 10 ml of Dulbecco's modified Eagle medium (DMEM) containing 10% fetal bovine serum. Digested material was centrifuged at 2500rpm for 2min; re-suspended in 1ml of Neural Basal Media (NBM) containing 2% B27 and 0.25% Glutamax (All from Invitrogen (Carlsbad, CA, USA)); then triturated through three glass pipettes of decreasing diameter. After centrifugation as before, the pellet was re-suspended in 250 μl/cortex of supplemented NBM and filtered though a

$watermark-text

$watermark-text

$watermark-text

40μm cell strainer (BD Biosciences, Bedford, MA, USA). Microfluidic culture devices were obtained from Xona microfluidics (Temecula, CA, USA). After plasma bonding to glass coverslips, the devices were coated with poly-D-lysine (Sigma, St Louis, MO, USA) and mouse laminin (Cultrex, Lake Forest, CA, USA). Fifteen microliters of neuron-containing suspension were seeded in the soma channel. Incubation was at 37°C, 10% CO_2, in a humidified incubator.

A modified technique that reduces glial cell contamination was used for some experiments. Briefly, trypsin was replaced by 10units/ml of papain in phosphate buffered saline (PBS) for 15min at 37°C. The medium was changed to PBS with Ca^{++} and Mg^{++} containing 75mg/ml BSA, 75mg/ml trypsin inhibitor and 1mg/ml DNase I. After 5min, the medium was replaced by PBS without Ca^{++} and Mg^{++} containing 75mg/ml bovine serum albumin (BSA) and 75mg/ml trypsin inhibitor and the tissues were triturated by repeated pipetting through at 1ml pipet tip (Pipetman). After filtration though a 40μm cell strainer and centrifugation at 1000rpm for 10min at room temperature, the cells were resuspended in 5 ml of NBM, layered on top of 3ml of 4% BSA in NBM and centrifuged as above. The cell pellet was resuspended in 10μl per cortex of supplemented NBM. The cell density was adjusted to 10^6 cells/5μl and 5μl of suspension were seeded in the soma channel.

Preparation of fibrillar Alexa Fluor 488- and ATTO 550-labeled α-synuclein

Recombinant wild-type α-synuclein was expressed in *E. coli* strain BL21(DE3) (Stratagene, Santa Clara, CA, USA) and purified as described[18]. The fibrillar form of the protein was generated and labeled with NHS-ester Alexa Fluor 488 (Invitrogen, Carlsbad, CA, USA) or NHS-ester ATTO-550 (ATTO-TEC GmbH, Siegen, Germany) as described[12]. The fibrillar nature of α-synuclein was assessed using a Jeol 1400 transmission electron microscope following adsorption onto carbon-coated 200-mesh grids and negative staining with 1% uranyl acetate. The images were recorded with a Gatan Orius CCD camera (Gatan, Pleasanton, CA, USA).

Preparation of Alexa 555- labeled fibrillar Aß42 peptide and Alexa 555-labeled BSA

Primers 5'-CCCGGGAATTCCATATGGACGCGGAATTTCGCCATGATAGCGGC-3' and 5'-TCCGCGGGATCCCTACTATGCAATCACGACGCCTCCGACC-3' were used to amplify the Aß42 peptide with an N-terminal Met codon. Amplified DNA was cloned into the pET3a vector (Novagen) between the NdeI and BamH1 restriction sites and expressed in E. Coli. strain BL21(DE3) codon+ (Stratagene, Santa Clara, CA, USA). Recombinant Aß1-42 was purified as described[19]. Met-Aß1-42 was diluted in PBS to a concentration of 100μM and incubated at 37°C for 5 days. Fibrillar Met-Aß1-42 was labeled with Alexa 555 as described for fibrillar α-synuclein[12]. Aliquots were flash frozen in liquid nitrogen, and stored at -80°C. BSA (Sigma, St Louis, MO, USA), 1 mg/ml in PBS, was labeled with Alexa 555 and purified as described for fibrillar α-synuclein[12].

Immunostaining

Cells were incubated with Calcein AM and visualized live or incubated with Alexa Fluor 555-labeled cholera toxin B (both from Invitrogen, Carlsbad, CA, USA) for 30min then fixed with 4% paraformaldehyde in PBS and washed once with PBS. Antibodies were diluted in PBS containing 2% BSA, 2% normal goat serum and 0.2% Triton X-100. Anti-class III ß-tubulin (Neuromics, Edina, MN, USA) was diluted 1:1000. Anti-phosphorylated neurofilament, clone SMI 31 (Covance, Princeton, NJ, USA) was diluted 1:1000. Incubation with primary antibody was for 3hr followed by 5 washes in PBS and a 1hr incubation with a 1:1000 dilution of secondary antibodies (Invitrogen, Carlsbad, CA, USA). Incubations were at room temperature. Cells were covered with Vectashield containing DAPI (Vector Laboratories, Burlingame, CA) after 5 washes in PBS.

$watermark-text

$watermark-text

$watermark-text

Microscopy and spectral analysis

Confocal microscopy was done with a Leica SP2 microscope equipped with a UV-405 laser. For spectral analysis, a region of interest was selected and the emission intensity was measured in increments of 5nm. Leica application suite software was used for quantitation.

Live cell imaging was done with a Nikon Eclipse Ti inverted microscope (60x and 100x oil objectives). The microfluidic devices were maintained at 37°C with 10% CO_2 during acquisition at either 80ms time intervals for 80s or 500ms intervals for 250s. Time-series images were analyzed using Fiji software (http://fiji.sc/wiki/index.php/Fiji). Segments of axons that showed puncta movements were traced and kymographs were made for each region of interest. Average and maximum velocities of punctae were calculated from the kymographs.

Results

Uptake of α-synuclein fibrils by primary neurons

To determine whether primary cortical neurons could internalize purified α-synuclein fibrils, Alexa Fluor 488-labeled fibrils (Fig 1A) were added to the medium of one-week-old cultures to a final concentration of 6nM. After 24 hours, the cells were fixed, immunostained, and analyzed by confocal microscopy. Alexa Fluor 488 containing punctae could be readily identified within the cytoplasm of cells that expressed the neuronal marker β-III tubulin (Fig 1B), confirming results previously published by others[12-14]. The colocalization of fibrils and β-III tubulin demonstrated their cytoplasmic position. Both neuronal and non-neuronal cell types contained fibrillar α-synuclein (Fig 1B).

Anterograde axonal transport of α-synuclein fibrils

We utilized microfluidic devices[20], to separate neuronal cell bodies from their axons and from second-order neurons that would be contacted by those axons (Supplemental Fig 1). Fluidic isolation was achieved by maintaining a volume difference of 100μl between the soma and axon chambers. Isolation has been demonstrated previously [19]. We confirmed that isolation was achieved in our set up using a 30-nm virus, smaller than the α-synuclein fibrils (see Fig 1), and an extremely sensitive infectivity assay with a detection limit of 3 plaque forming units. We could not detect any infectivity in the opposite chambers after 32h of incubation (Supplemental Fig 1C).

Primary neurons were seeded on one side of such a microfluidic device and cultured for one week. Numerous extensions had entered the opposite channel through the 450-nm long microgrooves, as shown by adding Calcein AM to the culture. Immunolabeling with the anti-neurofilament antibody SMI 31 showed that these extensions were axons (Supplemental Fig 2).

To determine whether the α-synuclein fibrils could be transported along these axons in an anterograde direction, Alexa Fluor 488-labeled fibrils (Syn-488) were introduced into the chamber containing the neuron cell bodies together with Alexa Fluor 555-labeled cholera toxin B (CtB-555) to label cellular membranes. The microgrooves were observed by confocal microscopy after 4-5 hours of incubation. Fluorescent punctae were observed associated with axons (Fig 1C), strongly suggesting that fibrillar α-synuclein had arrived there by anterograde transport from the cell body.

We compared the emission spectra of punctae, in confocal optical sections, with those of the dyes used in the experiment. Figure 1D shows the emission spectrum of the punctum shown in Figure 1C, of Alexa Fluor 488-labeled fibrils alone, and of the green background

$watermark-text

$watermark-text

$watermark-text

autofluorescence observed in formaldehyde-fixed frozen brain sections. Brain was chosen as a control because no such background was observed in the primary neuron cultures. Figure 1D shows that the spectrum of the punctum within the axon was similar to that of the labeled fibrils and distinct from autofluorescence, arguing that such punctae correspond to fibrillar α-synuclein. The emission spectrum for cholera toxin B was the same for both the soma compartment and the structures that surrounded the punctum, arguing that the fibrils were surrounded by axonal membranes. Thus, the fibrils introduced in the soma compartment could be unambiguously identified, shown to be internalized by neurons and transported axonally in an anterograde direction.

Characterization of the axonal transport of α-synuclein fibrils

We quantified anterograde axonal transport of α-synuclein fibrils using live-cell imaging. The neuron isolation protocol was modified (Materials and Methods) to reduce the number of astrocytes and to increase the number of axons in the microgrooves. Using anti-ß-III tubulin and anti-GFAP antibodies we found that approximately 50% of the cells were neurons and 50% were astrocytes (not shown). In a typical culture approximately 600 axons emerged from the microgrooves after one week. ATTO550-labeled α-synuclein fibrils (1.5nM) were added to the soma compartment of such cultures and the movement of punctae was characterized 4-5 hr later. A large number of moving punctae were readily observed within the microgrooves as well in the axons in the axon channel (Fig 2A and Supplemental Movies 1 and 2).

To characterize the movements of punctae in axons, images were collected at 80ms or 500ms intervals, depending on the experiment, for up to 500s. The velocity of punctae was measured along a defined region of interest (ROI) of an axon, as shown in Figure 2B and displayed as kymographs (Fig 2C, D). A total of 52 punctae on 26 axonal segments were analyzed. Images from the microgrooves allowed unambiguous distinction between anterograde and retrograde movements. Three types of movement were observed: a steady anterograde movement with an average velocity of 163μm/min, consistent with fast axonal transport (Fig 2D); punctae moving at a similar velocity but pausing for various lengths of time between phases of movement (Fig 2D); finally punctae with complex kinetics that displayed periods of movement at various velocities and periods of rest (Fig 2C). Overall these kinetics are characteristic of slow component-b of axonal transport[16,17]. On occasion, as in Figure 2D, a punctum was observed moving in a retrograde direction. Some punctae were immobile during the whole recording (Fig 2A and Supplemental Movies 1 and 2).

The signal to noise ratio (SNR) for fluorescence intensity of punctae was used as a measure of size since the molecules of α-synuclein were uniformly labeled with a covalently linked fluorochrome. We observed a moderate negative association between both maximum and average velocity and SNR (Fig 3). Small punctae displayed a large range of velocities up to a maximum of around 400μm/min. Their average and maximum velocities were nearly identical, which demonstrates that they did not pause during recording. The velocity of large punctae decreased as their size increased. The decrease of average velocity resulted from both decreased maximum velocity and a larger number, and/or length, of pauses.

Transmission of α-synuclein fibrils to second-order neurons following anterograde axonal transport

We tested whether α-synuclein fibrils could be transmitted to second-order neurons following anterograde transport. Neurons cultured in one channel were allowed to extend axons in the opposite channel for one week. α-Synuclein fibrils were then added to the soma of these neurons and, at the same time, freshly isolated neurons were added to the axonal compartment to serve as potential recipient cells (Fig 4C). A volume excess of 100μl was

$watermark-text

$watermark-text

$watermark-text

maintained in the recipient neuron chamber. After 4 days, fluorescent punctae were readily observed in recipient cells (Fig 4D). Staining with an anti ßIII-tubulin antibody and confocal microscopy showed that both neurons and non-neuronal cells had internalized axonally transported α-synuclein fibrils (Fig 4D). Colocalization between punctae and β-III tubulin demonstrated their intracytoplasmic localization in neurons. As a control for a possible retrograde transport of α-synuclein fibrils into the soma of the recipient neurons, fibrils and neurons were introduced into opposite chambers of an empty device and the culture was incubated for four days. A volume excess of 100μl was maintained in the chamber with neurons (Fig 4A). As illustrated in Figure 4B, no background retrograde transport to the recipient neurons was observed. We therefore conclude that fibrillar α-synuclein can be transferred to the cell body of second-order neurons following anterograde transport.

We used the modified protocol for neuron culture to measure the efficiency of axon to recipient cell transfer more precisely. The setup of the experiment was as shown in Figure 4C except that after adding fibrils in the first neuron channel and recipient neurons in the other channel, the culture was continued for only 24hr, then fixed and reacted with an anti-ßIII-tubulin antibody. The total number of fluorescent, fibril-containing cells in the recipient channel was determined by systematically scanning the entire channel with a 45x objective. In the experiment described in Figure 4E, there were 572 such cells. Twenty to 24 fields that contained positive cells in both the first neuron channel and the recipient channel were selected and examined by confocal microscopy to determine the percentage of fibril-containing cells that were neurons. Out of 483 and 572 fibril positive cells examined in the first neuron channel and the recipient channel, respectively, approximately 50% were neurons (Fig 4E). The other half must have been astrocytes since these cultures are made of 50% neurons and 50% astrocytes.

Finally, we examined if the fibrillar form of the Aß42 peptide, associated with Alzheimer disease, behaved in the same way as α-synuclein in the microfluidic device. Bovine serum albumin (BSA) was also tested as a control soluble protein. Both proteins were labeled with Alexa-555 fluorochrome in parallel with α-synuclein and run in parallel in an experiment analogous to that shown in Figure 4. Interestingly, after 24h of incubation, the Aß42 peptide fibrils gave punctae that appeared in neurites of the first neurons (Supplemental Figure 3A), and in axons both in the microgrooves and the axon channel (Supplemental Figure 3B,C). Some rare punctae were observed in the soma of second-order neurons (not shown). BSA, on the other hand, although it may have been internalized by neurons (Supplemental Figure 3D), was not detected in axons in the axon channel or in second-order neurons (not shown).

Discussion

In this study, we demonstrate that α-synuclein fibrils are internalized, anterogradely transported within axons, released, and subsequently taken up by additional neurons. Transfer of α-synuclein fibrils to neuronal soma following axonal transport may explain the characteristic pattern of spread of Lewy bodies between anatomically connected brain areas, in particular from the limbic system to the neocortex where misfolding of α-synuclein is responsible for PD-associated dementia. Although the mechanism of lesion formation following such axonal transport and uptake is outside the scope of our study, there is accumulating evidence that α-synuclein fibrils might behave as prions and seed the misfolding of endogenous α-synuclein[3-8]. Therefore, the data presented here may explain an important aspect of PD pathogenesis.

The punctae present in axons were of various sizes, which appeared to influence the rate of their transport. An analysis of velocity as a function of size shows that both maximum velocity and average velocity decreased as punctum size increased. More surprising was the

$watermark-text

$watermark-text

$watermark-text

observation that small punctae showed a large range of velocities that extends from 10μm/min to 400μm/min (Fig 3). Since the average velocity of many of these punctae was equal to their maximum velocity, this variation cannot be explained by pauses of varying length, at least at a level that could be detected under our conditions. This type of movements corresponds to what has been described as slow component-b of axonal transport[16,17]. Interestingly, endogenous, soluble α-synuclein, is transported as part of a large cargo of many different proteins with kinetics that also correspond to slow component-b[16,17,21,22]. Our results may indicate that, following internalization by soma or dendrites, fibrillar α-synuclein finds its way into the pathways that address cargo of iterative protein complexes to the axon hillock and the microtubule-dependent machinery responsible for this class of transport.

Interestingly, uptake by neuron soma and anterograde axonal transport was also observed for fibrils of Aß42 peptide, but not for a soluble protein (BSA) (Supplemental Figure 3). Our observation with the Aß42 peptide may have important implications for the pathogenesis of Alzheimer disease. However, this is outside of the scope of the present article. The similar behavior of α-synuclein and Aß42 fibrils indicates that axonal transport of protein assemblies is not necessarily determined by the nature of the proteins but rather by the repetitive nature of the cargo. The efficiency of transfer of α-synuclein fibrils from axons to a second-order neuron appears to be low, although the experimental set up did not allow for a real measurement of efficiency. In the experiment described in Figure 4, fluorescent punctae were found in 286 of the 5×10^5 second-order neurons introduced in the channel. Obviously, such ratio depends on the number of second-order neurons, which was arbitrary. It may be more telling to consider that the punctae that were observed in approximately 300 neurons and 300 glial cells after 24h had been introduced into the second-neuron channel by approximately 600 axons.

The mechanism of exit of fibrillar α-synuclein from axons and of uptake by neuronal soma deserves close examination. In particular the respective roles of axonal lysis and of unconventional secretion in exit, and the role of synaptic contacts in transfer, remain to be more directly investigated. Our findings suggest that transfer can occur in the absence of synapses since their formation in mixed E17 murine neuron/astrocyte cultures requires 2 to 3 weeks (Ben Barres, personal communication), whereas the second order-neurons had been cultivated for only 1 or 4 days, depending on the experiment. Also, we observed that the axons emerging from the microgrooves and the second neurons were not in the same plane. Axons tend to adhere to the PDMS “ceiling” of the channel whereas the recipient neurons and astrocytes adhered to the glass “floor”, the two being separated by 100μm (Supplemental Figure 4). Therefore, our results suggest that fibrillar α-synuclein exited the axons and entered the extracellular milieu prior to cellular uptake. If axon-to-soma transmission of misfolded α-synuclein occurs by a similar mechanism in the CNS, this extracellular step may represent an opportunity to intercept fibrillar α-synuclein with drugs which could inhibit the progression of PD and other synucleinopathies.

Supplementary Material

Refer to Web version on PubMed Central for supplementary material.

Acknowledgments

We thank Ben Barres and Daniel Dunia for advice, David Schneider for lending equipment, and Ben Barres, Peter Sarnow, and Larry Steinman for critical reading of the manuscript. E.C.F. was supported by an NIH NRSA fellowship. N.M. acknowledges support from the Ruth L. Kirstein National Research Service Award 1F32GM090545 from NIH. E.K.C. was supported by a Stanford University School of Medicine Dean's Postdoctoral Fellowship. L.B., Y.S. and R.M. were supported by Agence Nationale de la Recherche (ANR-08-

NEUR-001-01 and ANR-09-MNPS-013-01), the CNRS and the Fondation Bettencourt-Scueller. M.C. acknowledges support from NIH Grant 5R00CA125994. M.B. and K.K acknowledge support from NIH grant AI-65972, The Michael J. Fox Foundation for Parkinson's Research and a NIH Director's Pioneer Award DP1 827 to K.K.

REFERENCES

1. Lees AJ. The Parkinson chimera. Neurology. 2009; 72:S2–S11.2. [PubMed: 19221309]
2. Stefanis L. Alpha-synuclein in Parkinson's disease. Cold Spring Harb Perspect Med. 2012; 4:a009399. [PubMed: 22355802]
3. Brundin P, Li JY, Holton JL, Lindvall O, Revesz T. Research in motion: the enigma of Parkinson's disease pathology spread. Nat Reviews Neurosci. 2008; 9:741–745.
4. Goedert M, Clavaguera F, Tolnay M. The propagation of prion-like protein inclusions in neurodegenerative diseases. Trends Neurosci. 2010; 33:317–325. [PubMed: 20493564]
5. Conway KA, Harper JD, Lansbury PT. Accelerated in vitro fibril formation by a mutant alpha-synuclein linked to early-onset Parkinson disease. Nat Med. 1998; 4:1318–1320. [PubMed: 9809558]
6. Olanow CW, Prusiner SB. Is Parkinson's disease a prion disorder? Proc Natl Acad Sci USA. 2009; 106:12571–12572. [PubMed: 19666621]
7. Mougenot AL, Nicot S, Bencsik A, Morignat E, Verchère J, Lakhdar L, Legastelois S, Baron T. Prion-like acceleration of a synuclinopathy in a transgenic mouse model. Neurobiol Aging. 2011 (in press).
8. Luk KC, Kehm VM, Zhang B, O'Brien P, Trojanowski JQ, Lee VM. Intracerebral inoculation of pathological alpha-synuclein initiates a rapidly progressive neurodegenerative alpha-synucleopathy in mice. J Exp Med. 2012; 209:975–986. [PubMed: 22508839]
9. Braak H, Del Tredici K, Rüb U, de Vos RA, Jansen Steur EN, Braak E. Staging of brain pathology related to sporadic Parkinson's disease. Neurobiol Aging. 2003; 24:197–211. [PubMed: 12498954]
10. Kordower JH, Chu Y, Hauser RA, Freeman TB, Olanow CW. Lewy body-like pathology in long-term embryonic nigral transplants in Parkinson's disease. Nat Med. 2008; 14:504–506. [PubMed: 18391962]
11. Li JY, Englund E, Holton JL, Soulet D, Hagell P, Lees AJ, Lashley T, Quinn NP, Rehncrona S, Björklund A, Widner H, Revesz T, Lindvall O, Brundin P. Lewy bodies in grafted neurons in subjects with Parkinson's disease suggest host-to-graft disease propagation. Nat Med. 2008; 14:501–503. [PubMed: 18391963]
12. Hansen C, Angot E, Bergström AL, Steiner JA, Pieri L, Paul G, Outeiro TF, Melki R, Kallunki P, Fog K, Li JY, Brundin P. α-Synuclein propagates from mouse brain to grafted dopaminergic neurons and seeds aggregation in cultured human cells. J Clin Invest. 2011; 121:715–725. [PubMed: 21245577]
13. Desplats P, Lee HJ, Bae EJ, Patrick C, Rockenstein E, Crews L, Spencer B, Masliah E, Lee SJ. Inclusion formation and neuronal cell death through neuron-to-neuron transmission of α-synuclein. Proc Natl Acad Sci USA. 2009; 106:13010–13015. [PubMed: 19651612]
14. Luk KC, Song C, O'Brien P, Stieber A, Branch JR, Brunden KR, Trojanowski JQ, Lee VM. Exogenous α-synuclein fibrils seed the formationof Lewy body-like intracellular inclusions in cultured cells. Proc Natl Acad Sci USA. 2009; 106:20051–20056. [PubMed: 19892735]
15. Danzer KM, Ruf WP, Putcha P, Joyner D, Hashimoto T, Glabe C, Hyman BT McLean PJ. Heat-shock protein 70 modulates toxic extracellular α-synuclein oligomers and rescues trans-synaptic toxicity. The FASEB J. 2011; 25:326–336.
16. Roy S, Winton MJ, Black MM, Trojanowski JQ, Lee VM. Rapid and intermittent cotransport of slow component-b proteins. The J Neurosci. 2007; 27:3131–3138.
17. Roy S, Winton MJ, Black MM, Trojanowski JQ, Lee VM. Cytoskeletal Requirements in Axonal Transport of Slow Component-b. The J Neurosci. 2008; 28:5248–5256.
18. Ghee M, Melki R, Michot N, Mallet J. PA700, the regulatory complex of the proteasome, interferes with α-synuclein assembly. FEBS J. 2005; 272:4023–4033. [PubMed: 16098186]

$watermark-text $watermark-text $watermark-text

19. Walsh DM, Thulin E, Minogue AM, Gustavsson N, Pang E, Teplow DB, Linse S. A facile method for expression and purification of the Alzheimer's disease-associated amyloid beta-peptide. FEBS J. 2009; 276:1266–81. [PubMed: 19175671]

20. Taylor AM, Blurton-Jones M, Rhee SW, Cribbs DH, Cotman CW, Jeon NL. A microfluidic culture platform for CNS axonal injury, regeneration and transport. Nat Methods. 2005; 2:599–605. [PubMed: 16094385]

21. Utton MA, Noble WJ, Hill JE, Anderton BH, Hanger DP. Molecular motors implicated in the axonal transport of tau and alpha-synuclein. J Cell Sci. 2005; 118:4645–4654. [PubMed: 16176937]

22. Tang Y, Das U, Scott DA, Roy S. The slow axonal transport of alpha-synuclein. Mechanistic Commonalities Amongst Diverse Cytosolic Cargoes. Cytoskeleton. 2012 doi: 10.1002/cm.21019.

$watermark-text

$watermark-text

$watermark-text

$watermark-text
$watermark-text
$watermark-text

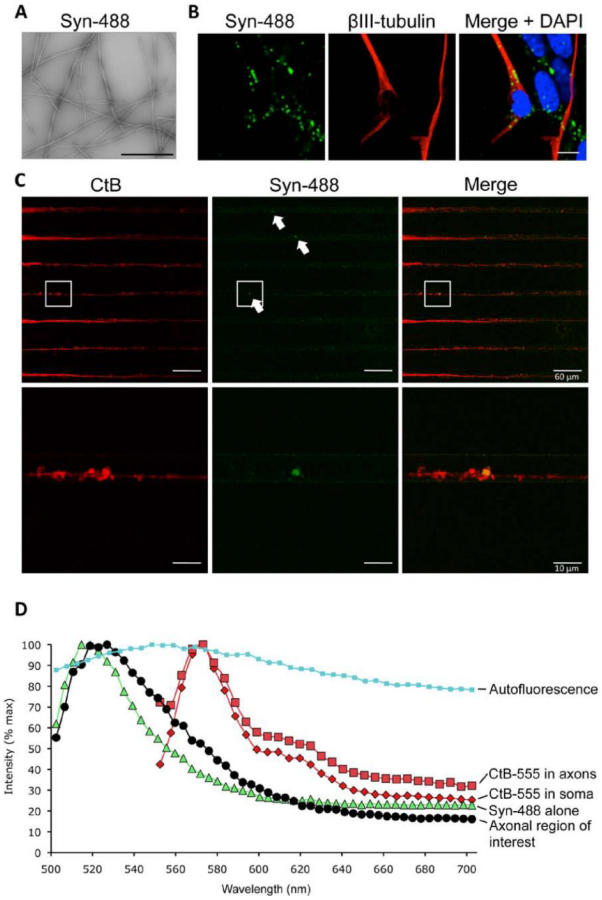

Figure 1.

Internalization and anterograde axonal transport of α-synuclein by primary neurons. (A) Alexa Fluor 488-labeled α-synuclein fibrils (Syn-488) were imaged by transmission electron microscopy. Scale bar = 200nm. (B) Fibrils were added to primary cortical neurons and incubated for 24 hours. Cells were reacted with an anti-ß-III tubulin antibody to identify neurons, stained with DAPI to identify nuclei and observed by confocal microscopy. Scale bars = 10μm. (C) Anterograde axonal transport of α-synuclein fibrils. Alexa Fluor 488-labeled fibrillar α-synuclein (Syn-488) and Alexa Fluor 555-labeled cholera toxin subunit B (CtB) were added to the soma of cortical neurons in a microfluidic device. A volume difference was maintained to prevent passive diffusion of fibrillar α-synuclein into the opposite chamber. Axons within microgrooves were visualized by confocal microscopy. Areas of green fluorescence are indicated by arrows. The lower panel shows higher magnification of the boxed region. (D) Emission spectra of the regions of interest (box) shown in C. Spectra were compared with those of pure Syn-488 deposited on a microscope slide and of the red fluorescence in soma and axons (CtB-555). A typical autofluorescence signal was determined using an unrelated CNS tissue sample.

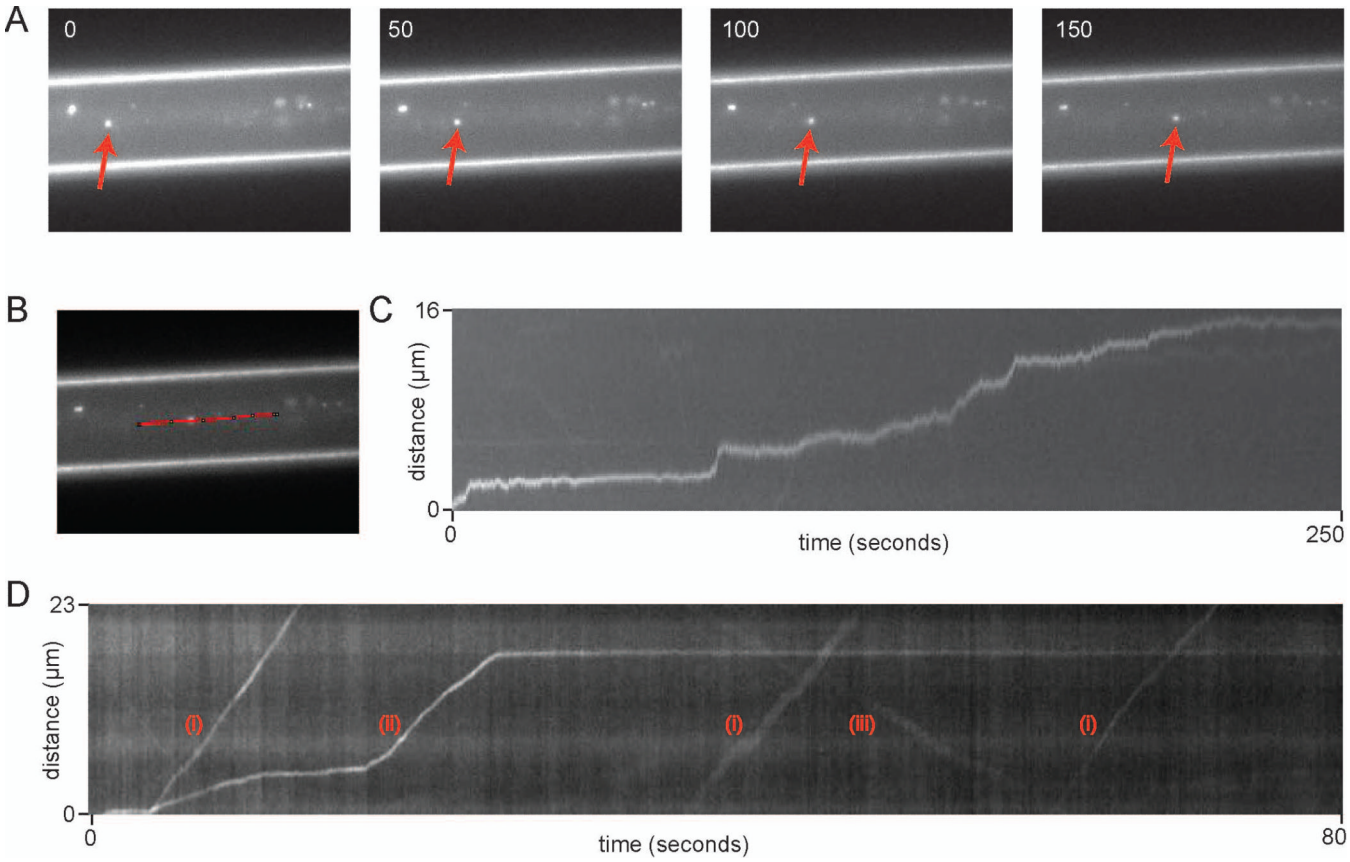

Figure 2.

Kinetics of axonal transport of α-synuclein fibrils. (A) Representative field of time-lapse analysis for an axon in a microgroove. The two bright lines correspond to the edges of the microgroove. The red arrow indicates the movement of a punctum through an axon. The time is given in seconds in the upper left hand corner of each image. Soma is to the left. (B) Selection of axon segment for velocity and flux measurements. (C) Kymograph of the punctum from (A) as it traveled through the axonal segment highlighted in (B) over a 250s time interval. (D) A kymograph showing a variety of punctum movements, including three punctae with fast-anterograde movement (I), one punctum with a saltatory movement with a long pause (II), and one punctum that appears to move in a retrograde direction (III).

$watermark-text $watermark-text $watermark-text

$watermark-text
$watermark-text
$watermark-text

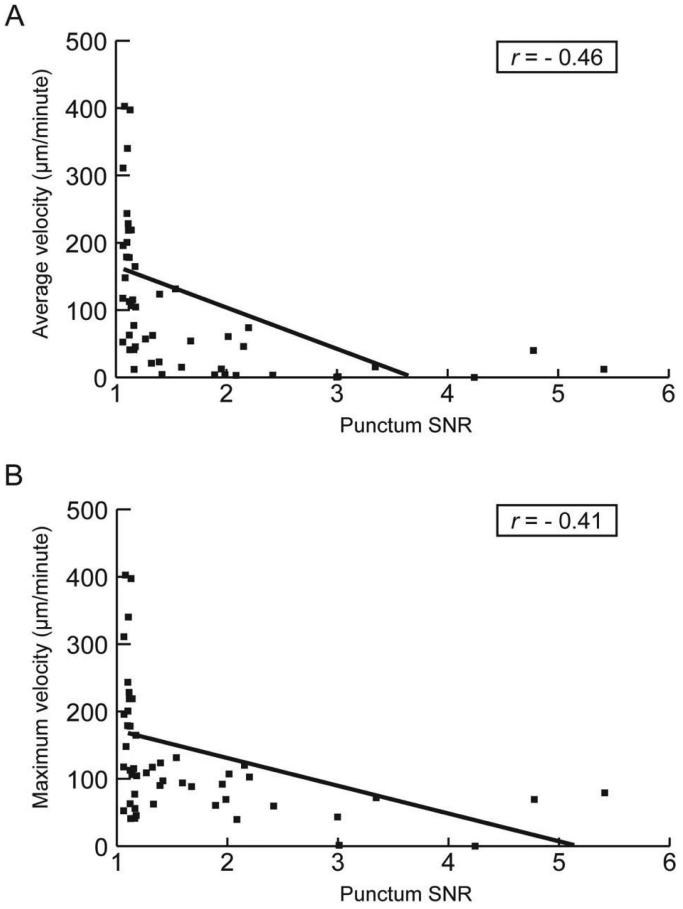

Figure 3.

Relationship between the velocity of punctae and their size. (A) The average velocity is plotted against the signal-to-noise ratio (SNR) of the fluorescence of each punctum. (B) The maximum velocity is plotted against the SNR for each punctum. The Pearson product-moment correlation coefficient (*r*) and the linear association trend line are shown for both (A) and (B).

$watermark-text
$watermark-text
$watermark-text

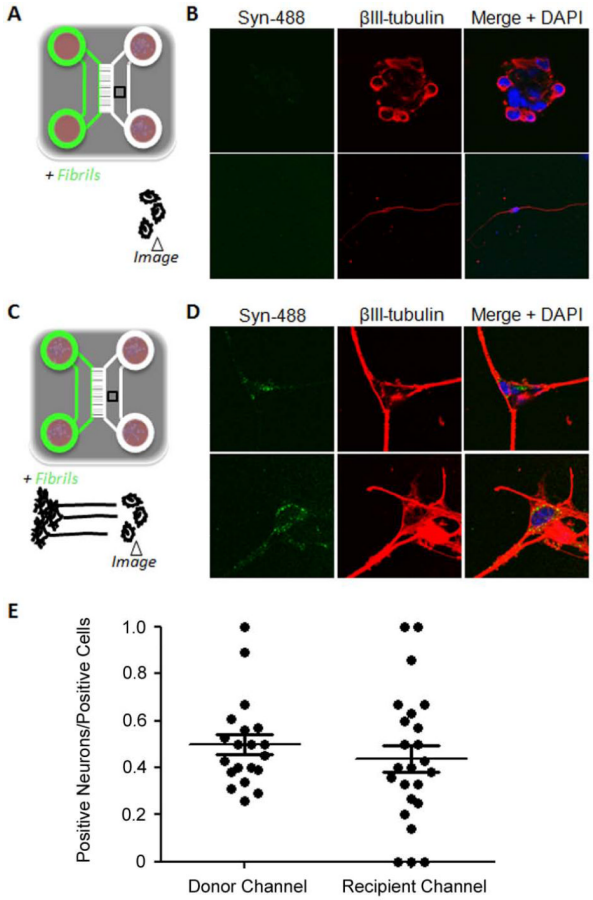

Figure 4.

Axonal transport and transmission of α-synuclein fibrils to second order neurons. (A) Set up of the control experiment to determine background retrograde transport. Syn-488 fibrils were added to one chamber that did not contain neurons. At the same time, recipient neurons were plated in the opposite channel that was given an additional 100μl of medium to prevent diffusion. (B) After four days of incubation the cells were stained with an anti-class III ß-tubulin (ßIII-tubulin) antibody to identify neurons and imaged by confocal microscopy. The upper and lower panels show two representative fields. (C) Schematic of the experimental setup to detect and measure transfer. Neurons were plated and cultured for one week to allow them to extend their axons to the opposite channel. At that time, Syn-488 fibrils were added to the chamber containing these neuron soma and freshly isolated neurons were added to the opposite channel. After one or four days in culture, depending on the experiment, the cells in both channels were stained with an anti-ßIII-tubulin antibody and analyzed by confocal microscopy. (D) The upper and lower panels show two representative fields. (E) For the experiments schematized in C, the percentages of Syn-488-positive cells that were neurons was determined by a blinded experimenter for the first neuron channel and the recipient channel. Graphs show individual values as well as mean ± SEM.